Electronic Supplementary Material (ESI) for Catalysis Science & Technology.
This journal is © The Royal Society of Chemistry 2020

Electronic Supplementary Information (ESI)

Deboronation-assisted construction of defective $Ti(OSi)_3OH$ species in MWW-type titanosilicate and their enhanced catalytic performance

Zhimou Tang [a], Yunkai Yu [a], Wei Liu [b], Zhen Chen [a], Rui Wang [a], Haoxin Liu [a], Haihong Wu [a], Yueming Liu *[a] and Mingyuan He [a]

[a] Shanghai Key Laboratory of Green Chemistry and Chemical Processes, School of Chemistry and Molecular Engineering, East China Normal University, North Zhongshan Rd. 3663, Shanghai 200062, P. R. China

[b] Shanghai Research Institute of Petrochemical Technology, SINOPEC, North Pudong Rd. 1658, Shanghai 201208, P. R. China

*Corresponding Author

Prof. Yueming Liu

Shanghai Key Laboratory of Green Chemistry and Chemical Processes, Department of Chemistry, East China Normal University, North Zhongshan Rd. 3663, Shanghai 200062, P. R. China

Tel: +86-21-6223-2058

Fax: +86-21-6223-2058

E-mail address: ymliu@chem.ecnu.edu.cn (Y.M. Liu)

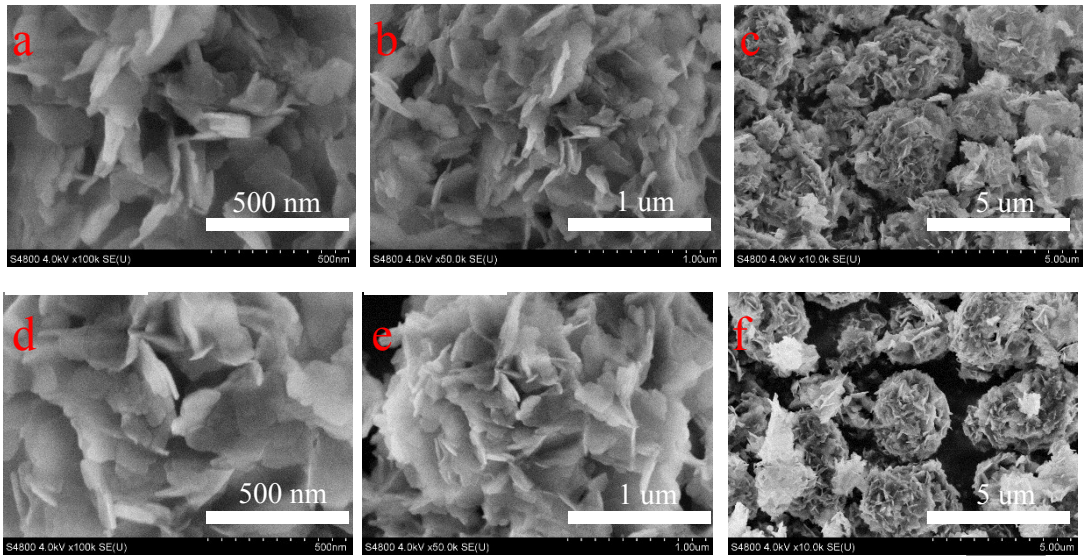

Fig. S1 SEM images of Ti-MWW(P)-C (a-c) and Ti-MWW(P)-AT-24 (d-f).

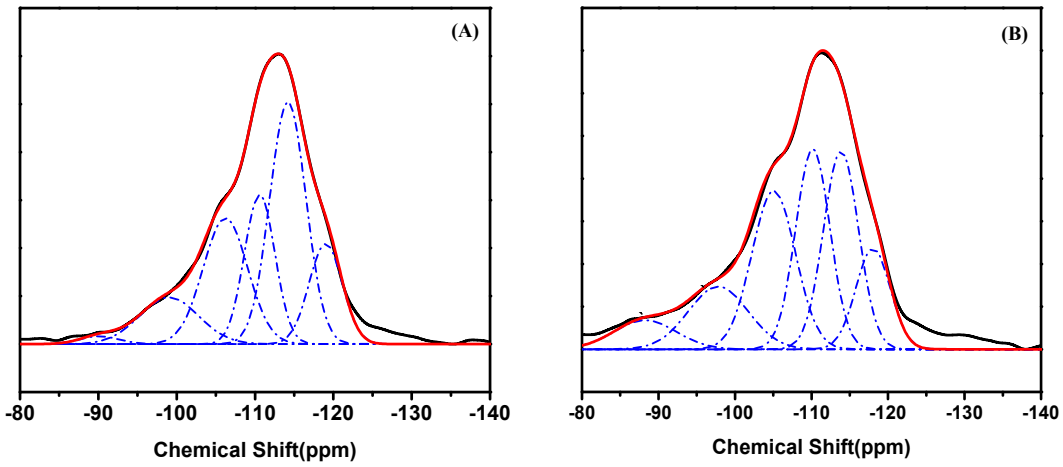

Fig. S2 ^{29}Si MAS NMR spectra of the Ti-MWW(P)-C (A), and Ti-MWW(P)-AT-24 (B). The black line is the experimentally recorded spectra, and the red line is the simulated spectra with the deconvoluted components between -90 and -130 ppm depicted blue.

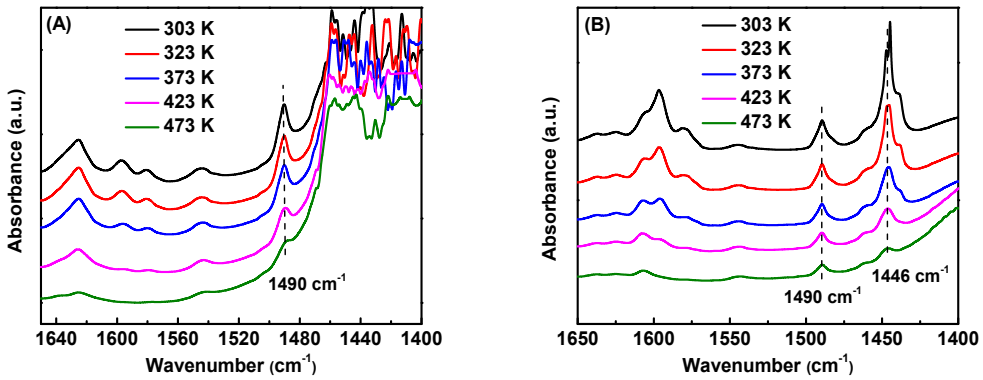

Fig. S3 FT-IR spectra in the pyridine regions of Ti-MWW(P)-C (A) and Ti-MWW(P)-AT-24 (B) at different evacuation temperatures.

It is observed that the signal of 1446 cm^{-1} is absent for Ti-MWW(P)-C, showing that there is little Lewis acidity in sample [1]. Based on the UV-Vis, UV-Raman and XPS analysis (Figure. 2A, B and C), it is clear that the extra-framework "TiO_6" species has an obviously negative effect on the framework "TiO_4" species, and the Lewis acidity of Ti-MWW(P)-C is therefore absent.

From the ^{11}B MAS NMR spectra and ICP measurement (Table 1 and Figure S5), it is deduced that there are large amounts of B(Ⅲ) species in Ti-MWW(P)-C. It is mentioned that the 1380 cm^{-1} band in IR spectra is assigned to the stretching vibration of Si-O-B bond from B(Ⅲ) species [2, 3]. Considering the absence of Lewis acidity as well as the existence of large amounts of B(Ⅲ) species, it is observed that the baseline of IR spectrum goes upward for Ti-MWW(P)-C in the region of over 1500 cm^{-1}. After the acid treatment, the boron content of Ti-MWW(P)-AT-x is low as indicated by the Si/B (> 36). More importantly, the alkaline pyridine molecular could promote the transformation of the remaining B(Ⅲ) species to B(Ⅳ) species [3-5]. Therefore, the band at 1380 cm^{-1} is absent for Ti-MWW(P)-AT-24.

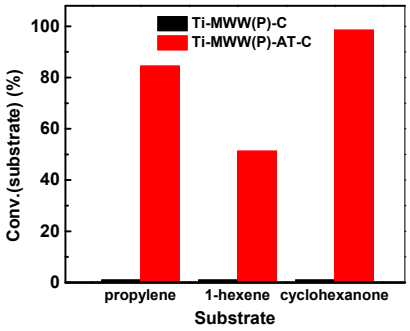

Fig. S4 Catalytic reactions of different substrate over Ti-MWW(P)-C and Ti-MWW(P)-AT-24.

Reaction condition in the epoxidation of propylene: catalyst 100 mg, propylene 30 mmol, H_2O_2 (30 wt.%) 30 mmol, CH_3CN 25 ml, temp 323 K, time 50 min.

Reaction condition in the epoxidation of 1-hexene: catalyst 50 mg, 1-hexene 10 mmol, H_2O_2(30 wt.%) 10 mmol, CH_3CN 10 ml, temp. 333 K, time 120 min.

Reaction condition in the cyclohexanone ammoximation: catalyst 150 mg, cyclohexanone 10 mmol, $NH_3 \cdot H_2O$ (25 wt.%) 17 mmol, H_2O_2 (30 wt.%) 11 mmol, *t*-BuOH (85 wt. %) 5000 mg, temperature 333 K, time 120 min.

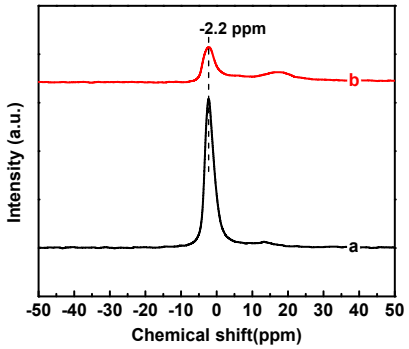

Fig. S5 ^{11}B MAS NMR spectra of Ti-MWW(P) (a) and Ti-MWW(P)-AT-24 (b).

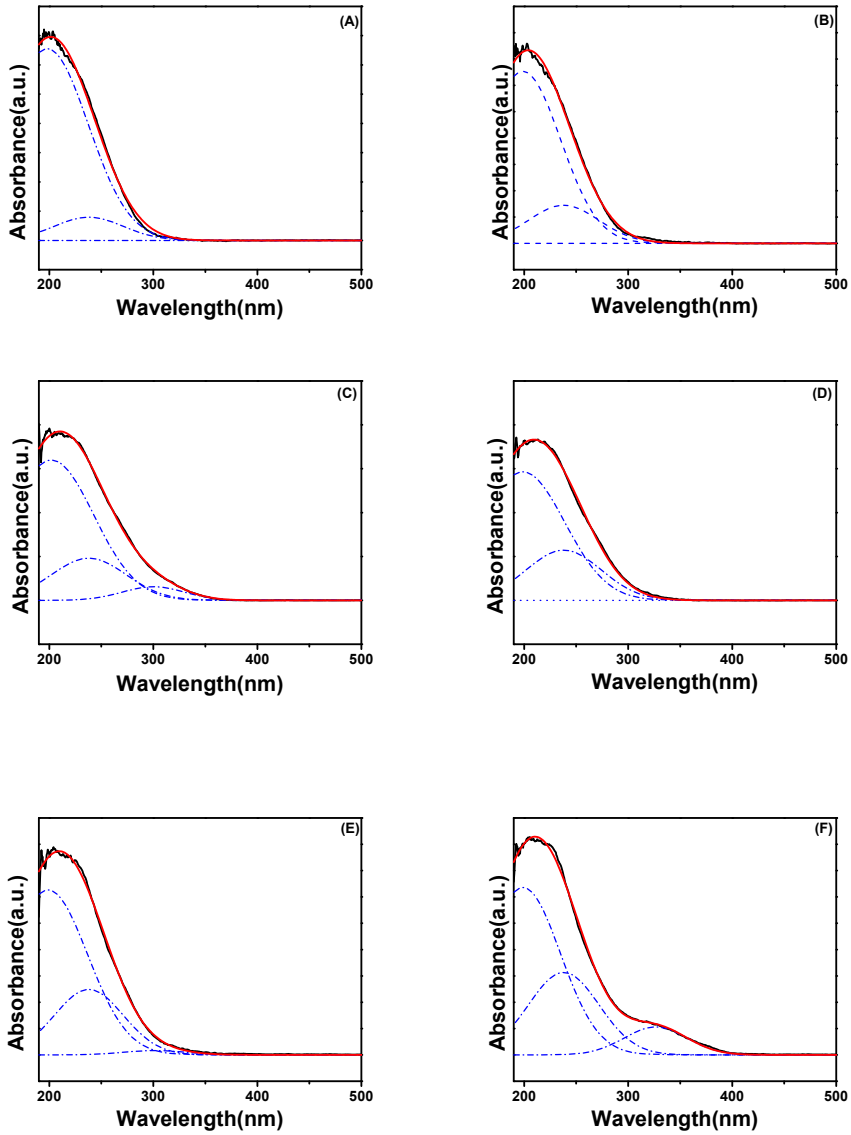

Fig. S6 UV-Vis spectra of Ti-MWW(P)-AT-x: Ti-MWW(P)-AT-2 (A), Ti-MWW(P)-AT-4 (B), Ti-MWW(P)-AT-8 (C), Ti-MWW(P)-AT-12 (D), Ti-MWW(P)-AT-16 (E), Ti-MWW(P)-AT-24 (F). The black line is the experimentally recorded spectra, and the red line is the simulated spectra with deconvoluted components at 210 nm, 230 nm, and 320 nm depicted blue.

The $Ti(OSi)_3OH$ species in Ti-MWW(P)-AT-x were quantified in UV/Vis spectra based on PeakFit program with the Gaussian fitting method [6]. Based on the previous studies [7, 8], the bands at 210 nm, 230 nm, and 320 nm are assigned to $Ti(OSi)_4$, $Ti(OSi)_3OH$, and TiO_2 species respectively. Hence, UV-Vis spectra of these samples were divided to three bands centered at around 210 nm, 230 nm, 320 nm, and their

corresponding FWHM in each sample is at the same level as far as possible. After the analysis of fitting results, it is found the FWHM of bands at 210 nm, 230 nm, 320 nm are ~90, ~80, and ~70 respectively, followed by the gradual increase of the percentage of $Ti(OSi)_3OH$ species (14.0% to 40.1%) (Fig. 5D in the text).

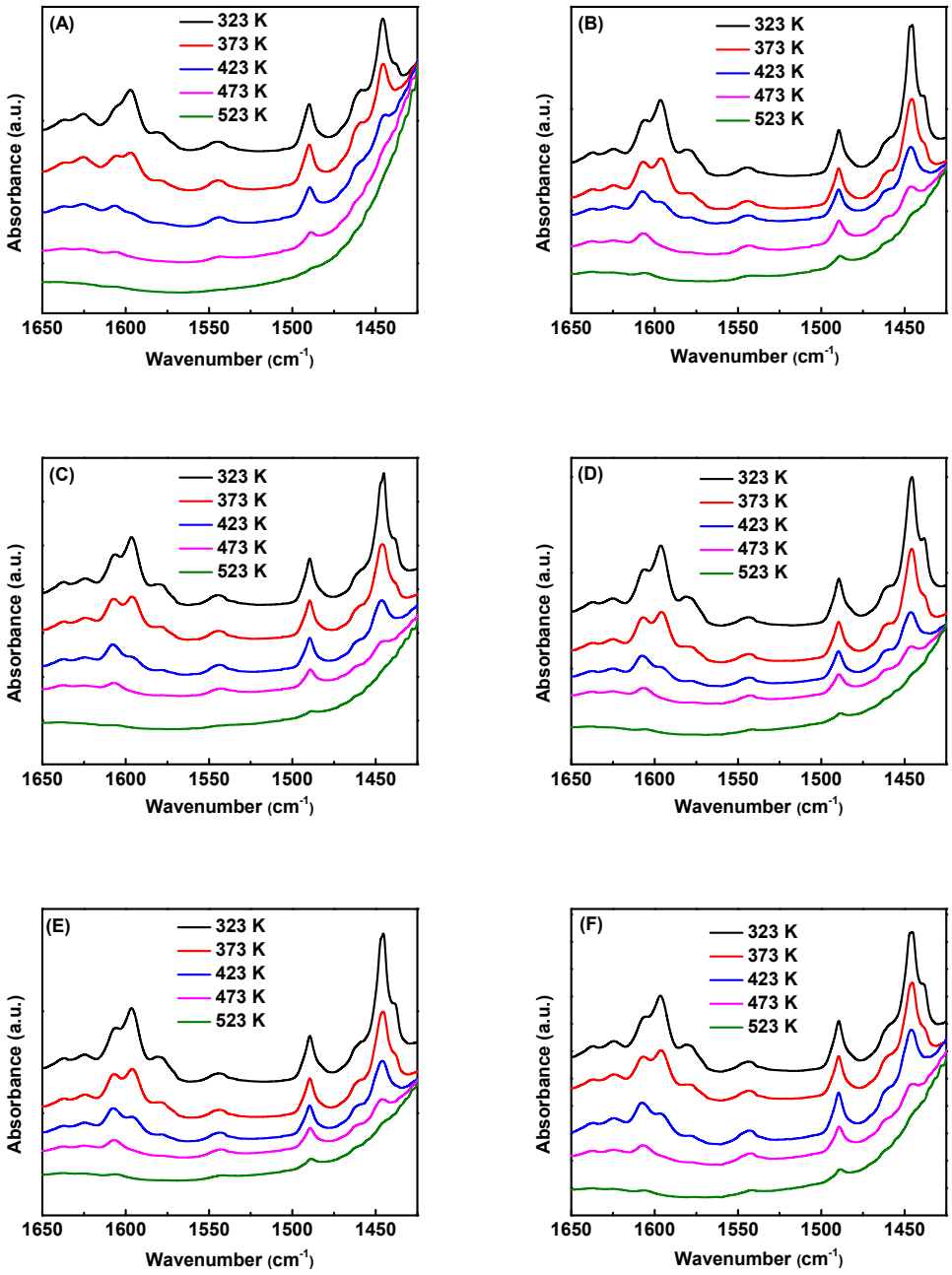

Fig. S7 FT-IR spectra in the pyridine regions at different evacuation temperatures over Ti-MWW(P)-AT-x: (A) Ti-MWW(P)-AT-2, (B) Ti-MWW(P)-AT-4, (C) Ti-MWW(P)-AT-8, (D) Ti-MWW(P)-AT-12, (E) Ti-MWW(P)-AT-16, (F) Ti-MWW(P)-AT-24.

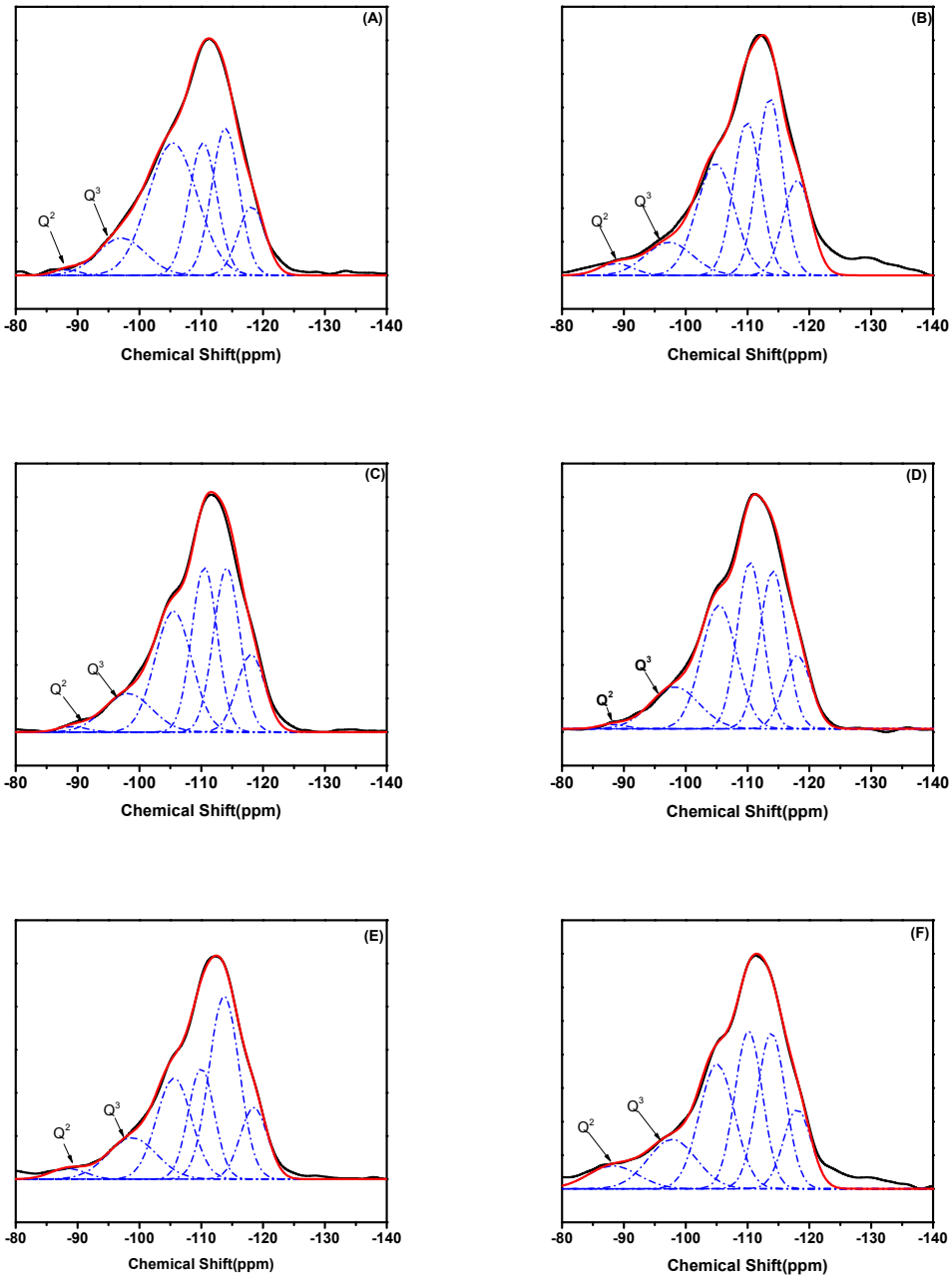

Fig. S8 ^{29}Si MAS NMR spectra of Ti-MWW(P)-AT-x: Ti-MWW(P)-AT-2 (A), Ti-MWW(P)-AT-4 (B), Ti-MWW(P)-AT-8 (C), Ti-MWW(P)-AT-12 (D), Ti-MWW(P)-AT-16 (E), Ti-MWW(P)-AT-24 (F). The black line is the experimentally recorded spectra, and the red line is the simulated spectra with deconvoluted components between -90 and -130 ppm depicted blue.

Table S1 A semiquantitative estimation for the number of $(SiOH)_4$ groups in Ti-MWW

Sample	A_{3500}[a]	A_{1880}[a]	Φ_{IR}[b]
Ti-MWW(P)-AT-2	20.507	23.524	0.872
Ti-MWW(P)-AT-4	22.127	21.892	1.011
Ti-MWW(P)-AT-8	16.059	22.595	0.711
Ti-MWW(P)-AT-12	21.063	24.118	0.873
Ti-MWW(P)-AT-16	16.697	21.351	0.782
Ti-MWW(P)-AT-24	15.612	21.799	0.716

[a] Integrated areas of the peak (3500 and 1880 cm^{-1}) in IR spectra.

[b] $A_{(SiOH)4}/A_{(Si\text{-}O\text{-}Si)}$

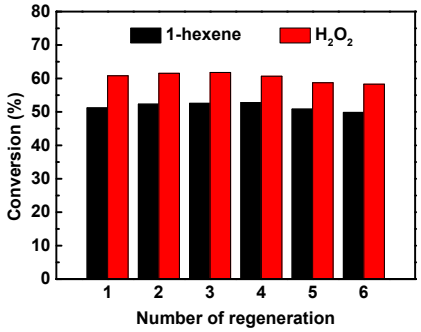

Fig. S9 Changes of conversion of 1-hexene and H_2O_2 with the reaction-regeneration cycles for Ti-MWW(P)-AT-24. Reaction conditions for the first run: catalyst 2000 mg, 1-hexene 400 mmol; H_2O_2(30 wt.%) 400 mmol; CH_3CN 400 mL; temp. 333 K; time 120 min. The next catalytic runs proceed at a constant ratio of catalyst–alkene-oxidant–solvent

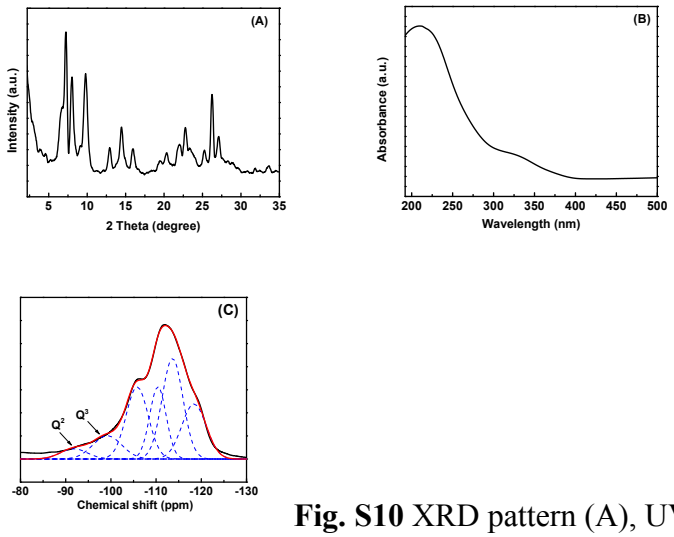

Fig. S10 XRD pattern (A), UV-Vis spectrum (B) and ^{29}Si MAS NMR spectrum (C) of the Ti-MWW-U.

Table S2 Catalytic performance for the epoxidation of 1-hexene with H_2O_2.

Sample	Si Concentration[a]	Si/Ti[a]	Si/B[a]	Conv. (1-hex.)/%[b]	Conv. (H_2O_2)/%[b]	Eff. (H_2O_2)/%[b]	Sel. (Epo.)/%[b]	TON[c]
Ti-MWW(P)-C	-	29	12	0	0	0	0	0
Ti-MWW(P)-AT-24	140	44	48	51.2	60.8	84.2	100.0	284
Ti-MWW-(B)	100	55	17	12.2	24.0	50.6	100.0	82

[a] Measured by ICP.

[b] Reaction conditions: catalyst 50 mg; 1-hexene 10 mmol; H_2O_2(30 wt.%) 10 mmol; CH_3CN 10 mL; temp. 333 K; time 120 min.

[c] In mol (mol.Ti)$^{-1}$.

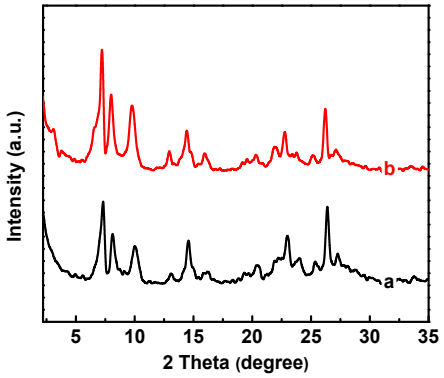

Fig. S11 Powder XRD patterns of Ti-MWW-(B) (a) and Ti-MWW(P)-AT-24 (b).

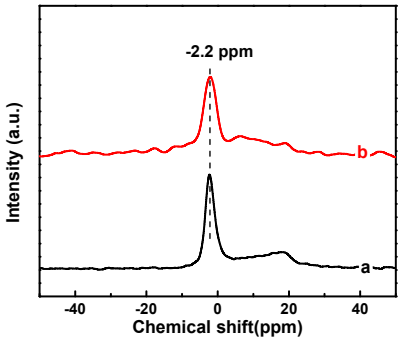

Fig. S12 ^{11}B MAS NMR spectra of Ti-MCM-56-AT-C (a) and Re-Ti-MCM-56(P)-AT-C (b).

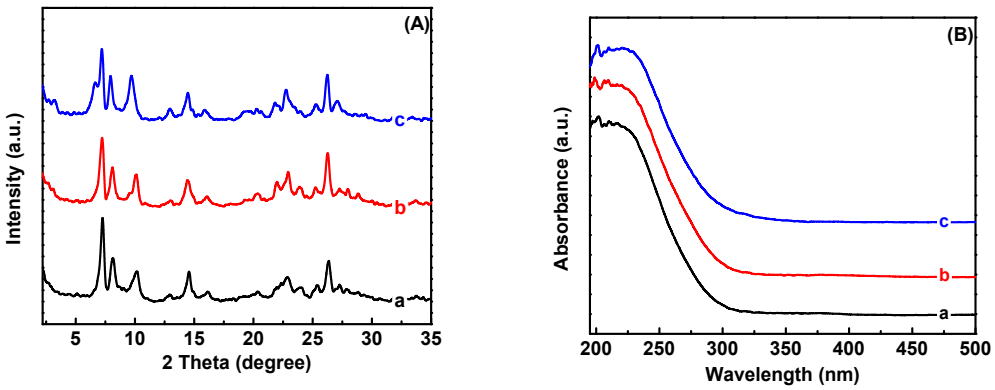

Fig. S13 XRD patterns (A) and UV-Vis spectra (B) of Ti-MWW(P)-AT-x with the control of acid-treated time: (a) 4h, (b) 8h, (c) 20h. The Si/Ti ratio of Ti-MWW(P) in this batch is 60.

Table S3 Catalytic performance for the epoxidation of 1-hexene with H_2O_2. [a]

Sample[b]	Si/Ti[c]	Si/B[c]	Conv. (1-hex.)/%	Conv. (H_2O_2)/%	Eff. (H_2O_2)/%	Sel. (Epo.)/%	TON[d]
Ti-MWW(P)-AT-4	86	62	10.8	18.1	59.9	100.0	113
Ti-MWW(P)-AT-8	87	57	17.3	24.3	71.3	100.0	188
Ti-MWW(P)-AT-20	97	71	15.9	16.6	95.8	100.0	192

[a] Reaction conditions: catalyst 50 mg; 1-hexene 10 mmol; H_2O_2(30 wt.%) 10 mmol; CH_3CN 10 mL; temp. 333 K; time 120 min.

[b] The Si/Ti ratio of Ti-MWW(P) in this batch is 60.

[c] Measured by ICP.

[d] In mol $(mol.Ti)^{-1}$.

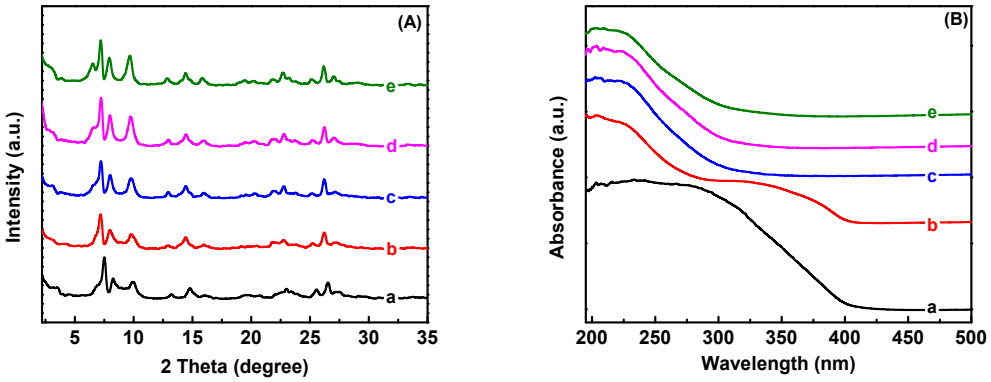

Fig. S14 XRD patterns (A) and UV-Vis spectra (B) of Ti-MWW(P)-AT with the control of acid-treated concentration: (a) 0.5 M, (b) 1.0 M, (c) 1.5 M, (d) 2.0 M, (e) 4.0 M.

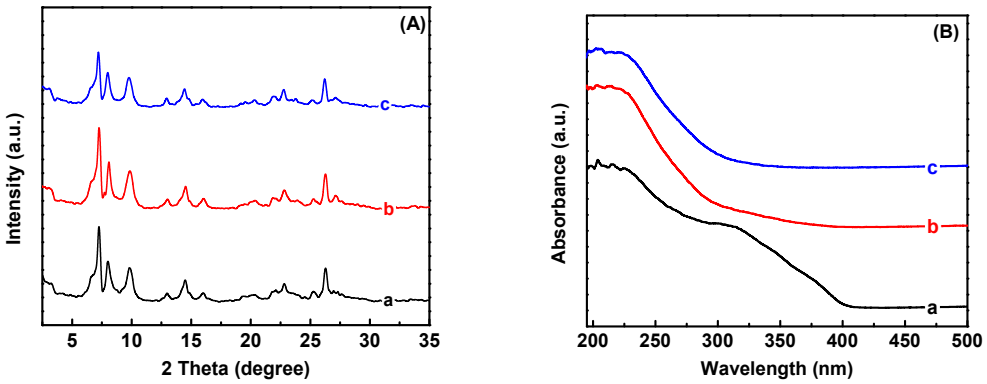

Fig. S15 XRD patterns (A) and UV-Vis spectra (B) of Ti-MWW(P)-AT with the control of acid-treated solid-to-liquid ratio: (a) 1:20, (b) 1:35, (c) 1:50.

Table S4 Catalytic performance for the epoxidation of 1-hexene with H_2O_2.

$C_{(HNO3)}$	Si/Ti[a]	Si/B[a]	Conv. (1-hex.)/%[b]	Conv. (H_2O_2)/%[b]	Eff. (H_2O_2)/%[b]	Sel. (Epo.)/%[b]	TON[c]
0.5 M	27	31	2.8	12.2	23.3	100.0	9
1.0 M	38	38	38.1	55.2	69.1	100.0	179
1.5 M	43	50	51.3	67.1	76.4	100.0	271
2.0 M	44	48	51.2	60.8	84.2	100.0	284
4.0 M	88	57	20.1	37.6	53.3	100.0	215

[a] Measured by ICP.

[b] Reaction conditions: catalyst 50 mg; 1-hexene 10 mmol; H_2O_2(30 wt.%) 10 mmol; CH_3CN 10 mL; temp. 333 K; time 120 min.

[c] In mol (mol.Ti)$^{-1}$.

Table S5 Catalytic performance for the epoxidation of 1-hexene with H_2O_2.

S/L ratio.	Si/Ti[a]	Si/B[a]	Conv. (1-hex.)/%[b]	Conv. (H_2O_2)/%[b]	Eff. (H_2O_2)/%[b]	Sel (Epo.)/%[b]	TON[c]
1:20	41	36	32.3	52.9	61.1	100.0	163
1:35	48	41	48.9	66.9	73.0	100.0	288
1:50	44	48	51.2	60.8	84.2	100.0	284

[a] Measured by ICP.

[b] Reaction conditions: catalyst 50 mg; 1-hexene 10 mmol; H_2O_2(30 wt.%) 10 mmol; CH_3CN 10 mL; temp. 333 K; time 120 min.

[c] In mol $(mol.Ti)^{-1}$.

Reference

1. Z. Zhuo, L. Wang, X. Zhang, L. Wu, Y. Liu and M. He, *J. Catal.*, 2015, **329**, 107-118.
2. J. Chen, T. Liang, J. Li, S. Wang, Z. Qin, P. Wang, L. Huang, W. Fan and J. Wang, *ACS Catal.*, 2016, **6**, 2299-2313.
3. R. De Ruiter, A. Kentgens, J. Grootendorst, J. Jansen and H. Van Bekkum, *Zeolites*, 1993, **13**, 128-138.
4. V. R. Marthala, W. Wang, J. Jiao, Y. Jiang, J. Huang and M. Hunger, *Micro. Meso. Mater.*, 2007, **99**, 91-97.
5. A. Hough, A. F. Routh, S. M. Clarke, P. V. Wiper, J. A. Amelse and L. Mafra, *J. Catal.*, 2016, **334**, 14-22.
6. A. J. Berry, L. V. Danyushevsky, H. S. C. O'Neill, M. Newville and S. R. Sutton, *Nature*, 2008, **455**, 960-963.
7. P. Ratnasamy, D. Srinivas and H. Knozinger, *Adv. Catal.*, 2004, **48**, 1-169.
8. W. Wang, G. Li, W. Li and L. Liu, *Chem. Commun.*, 2011, **47**, 3529-3531.